

Search for a heavy vector boson decaying to two gluons in $p\bar{p}$ collisions at $\sqrt{s} = 1.96$ TeV

We present a search for a new heavy vector boson Z' which decays to gluons, one of which is massive and splits to a pair of top quarks, leading to a final state of $t\bar{t}g$. In a sample of events with exactly one lepton, missing transverse momentum and at least five jets, corresponding to an integrated luminosity of 8.7 fb^{-1} collected by the CDF II detector, we find the data to be consistent with the standard model. We set cross-section upper limits on the production of this chromophilic Z' at 95% confidence level from 300 fb to 40 fb for Z' masses ranging from 400 GeV/c^2 to 1000 GeV/c^2 , respectively.

PACS numbers: 12.60.-i, 13.85.Rm, 14.80.-j

Models of physics beyond the standard model (SM) often predict new U(1) symmetries with an associated electrically neutral Z' gauge boson. Assuming coupling to charged lepton pairs, experiments at the LHC already rule out such particles up to masses of multiple TeV [21, 22]. Strict limits are also set by ATLAS and CMS in searches where the new particle decays to $t\bar{t}$ pairs [23, 24]. If the heavy new particle decays only to gluons, however, such limits are easily evaded. Such a scenario was examined in [1], where the chromophilic Z' predominantly via $Z' \rightarrow q\bar{q}g$.

In this paper, we consider the decay mode $Z' \rightarrow t\bar{t}g \rightarrow W^+bW^-\bar{b}g$ in which one W boson decays leptonically (including leptonic τ decays) and the second W boson decays to a quark-antiquark pair. This decay mode features large branching ratios while reducing to a manageable level the backgrounds other than SM $t\bar{t}$ production. Such a signal is similar to SM top-quark pair production and decay, but with an additional jet coming from the Z' resonance.

We analyze a sample of events corresponding to an integrated luminosity of $8.7 \pm 0.5 \text{ fb}^{-1}$ recorded by the CDF II detector [2], a general purpose detector designed to study $p\bar{p}$ collisions at $\sqrt{s} = 1.96$ TeV from the Fermilab Tevatron collider. CDF's tracking system consists of a silicon microstrip tracker and a drift chamber that are immersed in a 1.4 T magnetic field [3]. Electromagnetic and hadronic calorimeters surrounding the tracking system measure particle energies, with muon detector provided by an additional system of drift chambers located outside the calorimeters.

Events are triggered online by the requirement of an e or μ candidate [4] with transverse momentum p_T [5] greater than 18 GeV/c . After trigger selection, events are retained if the electron or muon candidate has a pseudorapidity $|\eta| < 1.1$ [5], $p_T > 20 \text{ GeV}/c$ and satisfies the standard CDF identification and isolation requirements [4]. We reconstruct jets in the calorimeter using the JETCLU [6] algorithm with a clustering radius of 0.4 in $\eta - \phi$ space, and calibrated using the techniques outlined in [7]. Jets are required to have transverse energy $E_T > 15 \text{ GeV}$ and $|\eta| < 2.4$. Missing transverse momen-

tum [8] is reconstructed using fully corrected calorimeter and muon information [4].

The signature of $Z' \rightarrow t\bar{t}g \rightarrow W^+bW^-\bar{b}g \rightarrow \ell\nu bqq'\bar{b}g$ is a charged lepton (e or μ), missing transverse momentum, two jets arising from b -quarks, and three additional jets from the two light flavor quarks and the Z' decay gluon. We select events with exactly one electron or muon, at least five jets, and missing transverse momentum greater than 20 GeV/c . Since a signal would have two jets with b -quarks, we require (with minimal loss of efficiency) evidence of decay of a b -hadron in at least one jet. This requirement, called b -tagging, makes use of the SECVTX algorithm [9].

We model the production of Z' with $m_{Z'} = 500 - 1000 \text{ GeV}/c^2$ and subsequent decays with MADGRAPH [10]. Additional radiation, hadronization and showering are described by PYTHIA [11]. The detector response for all simulated samples is modeled by the GEANT-based CDF II detector simulation [12].

The dominant SM background to the $t\bar{t} + j$ signature is top-quark pair production with an additional jet due to initial-state or final-state radiation. We model this background using PYTHIA $t\bar{t}$ production with a top-quark mass $m_t = 172.5 \text{ GeV}/c^2$, compatible with the best current determination [13]. We normalize the $t\bar{t}$ background to the theoretical calculation at next-to-next-to-leading order (NNLO) in α_s [14]. In addition, events generated by a next-to-leading order generator, MC@NLO [15] are also used in estimating an uncertainty in modeling the radiation of an additional jet.

The second largest SM background process is the associated production of a W boson and jets. Samples of W boson + jets events with light- and heavy-flavor jets are generated using ALPGEN [16], and interfaced with a parton-shower model from PYTHIA. The W boson + jets samples are normalized to the measured W boson production cross section, with an additional multiplicative factor for the relative contribution of heavy- and light-flavor jets, following the same technique utilized previously in measuring the top-quark pair-production cross section [9]. The multi-jet background, in which a jet is misreconstructed as a lepton, is modeled using a jet-

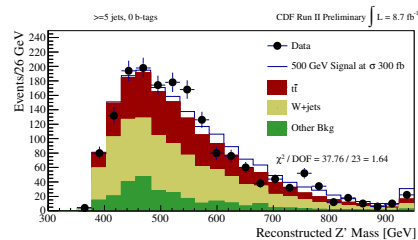
triggered sample normalized to a background-dominated region at low missing transverse momentum where the multi-jet background is large.

The SM backgrounds due to single top quark and diboson production are modeled using MADGRAPH interfaced with PYTHIA parton-shower models and PYTHIA, respectively, and normalized to next-to-leading-order cross sections [17].

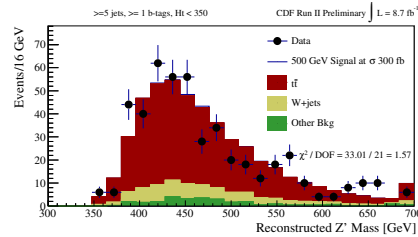
A signal may be observed as an excess of events above expectations from backgrounds in event distributions versus the mass of the $t\bar{t}j$ system ($Z' \rightarrow t\bar{t}j$). In $t\bar{t} + j$ events, we first identify the jets belonging to the $t\bar{t}$ system, using a kinematic fitter [18] to select from all available jets in the event the four jets most consistent with the $t\bar{t}$ topology. In the fit, the top-quark and W -boson masses are constrained to be $172.5 \text{ GeV}/c^2$ and $80.4 \text{ GeV}/c^2$, respectively. All remaining jets are considered candidates for the light-quark jet in the $t\bar{t}j$ resonance. Following the strategy proposed in Ref. [1], we choose the jet with the largest value of $\Delta R(j, t\bar{t}) \times p_T^{\text{jet}}$ to form the resonance-mass reconstruction, $m_{t\bar{t}j}$, where $\Delta R(j, t\bar{t})$ is the distance between a jet and the $t\bar{t}$ system in $\eta - \phi$ space. Backgrounds, in which there is no resonance, give a broad and low distribution of $m_{t\bar{t}j}$, while a signal would be reconstructed near the resonance mass.

We consider several sources of systematic uncertainty on the predicted background rates and distributions, as well as on the expectations for a signal. Each systematic uncertainty affects the expected sensitivity to new physics, expressed as an expected cross-section upper limit in the no-signal assumption. The dominant systematic uncertainty is the jet energy scale (JES) [7], followed by theoretical uncertainties on the cross sections of the background processes. To probe the description of the additional jet, we compare our nominal $t\bar{t}$ model to one generated by MC@NLO and take the full difference as a systematic uncertainty. We also consider systematic uncertainties associated with the description of initial- and final-state radiation [18], uncertainties in the efficiency of reconstructing leptons and identifying b -quark jets, and uncertainties in the contribution from multiple proton interactions. In addition, we consider a variation of the Q^2 scale of W boson+jet events in ALGPEN. In each case, we treat the unknown underlying quantity as a nuisance parameter and measure the distortion of the m_{tj} spectrum for positive and negative fluctuations of the underlying quantity. Table I lists the contributions of each of these sources of systematic uncertainty to the yields.

We validate our modeling of the SM backgrounds in three background-dominated control regions. The $t\bar{t}$ background is validated in events with exactly 4 jets and at least one b tag. We validate $W + \text{jets}$ backgrounds in events with at least 5 jets and no b tags. Finally, modeling of SM $t\bar{t}$ events with an additional jet is validated by examining a signal-depleted region with at least 5 jets, at least one b tag and H_T , the scalar sum of lepton and



(a) W boson + jet control region: at least 5 jets, exactly zero b -tags.



(b) $t\bar{t}$ plus additional radiated jet control region: at least 5 jets, at least one b -tag, $H_T < 350 \text{ GeV}$.

FIG. 1: Distribution of events versus reconstructed $t\bar{t}j$ invariant mass ($m_{t\bar{t}j}$) for observed data and expected backgrounds in two control regions. The lower panes give the relative difference between the observed and expected distributions; the hatched areas show the combined statistical and systematic uncertainties of the expected background.

TABLE I: Contributions to the systematic uncertainty on the two main expected background processes, the total background yield and an example $500 \text{ GeV}/c^2$ resonance signal with an assumed total cross section of 0.1 pb .

Process	$t\bar{t}$	$W + \text{jets}$	Total Bg.	Z'
Yield	550	79	670	34
JES	17%	15%	16%	9%
Cross section	10%	30%	12%	-
$t\bar{t}$ generator	6%	-	5%	-
ISR/FSR	6%	-	5%	4%
(e/μ , b -jet) ID eff.	5%	5%	5%	5%
Mult. interactions	3%	2%	3%	2%
Q^2 scale	-	19%	2%	-
Total syst. uncert.	22%	39%	22%	11%

jet transverse momenta, less than $350 \text{ GeV}/c$. As shown in Fig. 1, we find that the backgrounds are well modeled

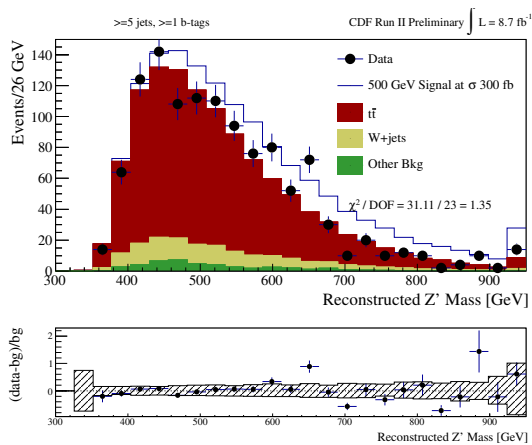


FIG. 2: Distribution of events versus reconstructed $t\bar{t}j$ invariant mass, $m_{t\bar{t}j}$, for observed data and expected backgrounds in the signal region. Three signal hypotheses are shown, assuming a total cross section of 0.1 pb. The lower pane gives the relative difference between the observed and expected distributions; the hatched area shows the combined statistical and systematic uncertainties of the expected background.

within systematic uncertainties.

Figure 2 shows the observed distribution of events in the signal region compared to possible signals and estimated backgrounds. We fit the most likely value of the sum of the Z' cross section by performing a binned maximum-likelihood fit in the $m_{t\bar{t}j}$ variable, allowing for systematic and statistical fluctuations via template morphing [19]. There is no evidence for the presence of top-quark-pair+jet resonances in $t\bar{t}j$ events, so we set upper limits on Z' production at 95% confidence level using the CLs method [20]. The observed limits are consistent with expectation in the background-only hypothesis (Fig. 3).

In conclusion, we report on the first search for top-quark-pair+jet resonances in $t\bar{t}j$ events. Such resonances are predicted by new physics models [1]. For each accepted event, we reconstruct the resonance mass ($m_{t\bar{t}j}$), and find the data to be consistent with SM background predictions. We calculate 95% CL upper limits on the cross section of such resonance production from X pb to Y pb for X masses ranging from 500 GeV/c^2 to 1000 GeV/c^2 and interpret the limits in terms of specific physics models. These limits constrain a small portion of the model parameter space. Analysis of collisions at the Large Hadron Collider may probe the remaining allowed regions.

We thank the Fermilab staff and the technical staffs of the participating institutions for their vital contributions. This work was supported by the U.S. Department of Energy and National Science Foundation; the Italian Istituto Nazionale di Fisica Nucleare; the Ministry of Education, Culture, Sports, Science and Technology of

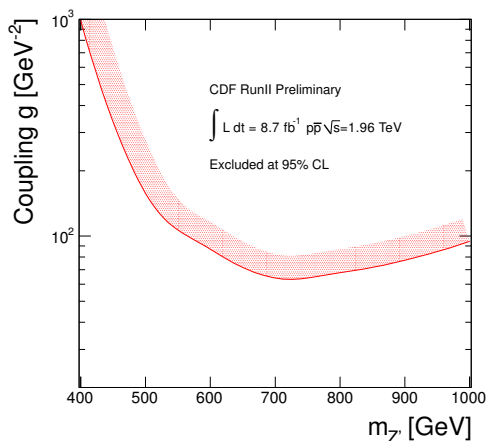
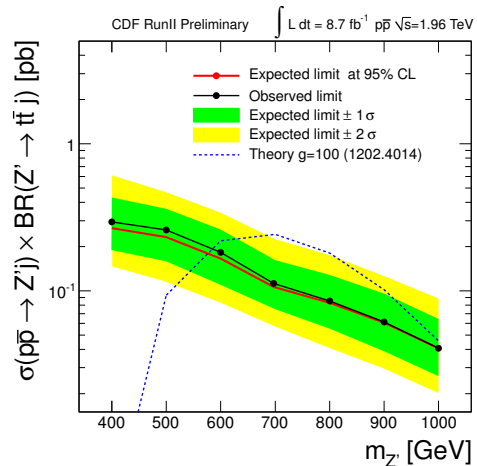


FIG. 3: Top, upper limits at 95% CL on $t\bar{t} + j$ production via a heavy new resonance Z' , as a function of the resonance mass. Bottom, limits on the coupling in the Z' theory versus resonance mass.

Japan; the Natural Sciences and Engineering Research Council of Canada; the National Science Council of the Republic of China; the Swiss National Science Foundation; the A.P. Sloan Foundation; the Bundesministerium für Bildung und Forschung, Germany; the Korean World Class University Program, the National Research Foundation of Korea; the Science and Technology Facilities Council and the Royal Society, UK; the Institut National de Physique Nucleaire et Physique des Particules/CNRS; the Russian Foundation for Basic Research; the Ministerio de Ciencia e Innovación, and Programa Consolider-Ingenio 2010, Spain; the Slovak R&D Agency; and the Academy of Finland.

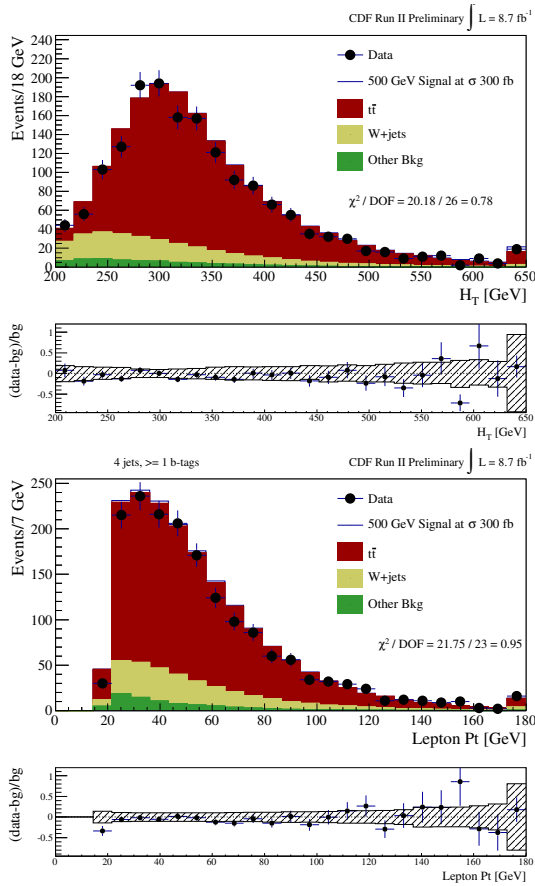


FIG. 4: Validation in the four jet control region: requiring exactly four jets and at least one b -tag.

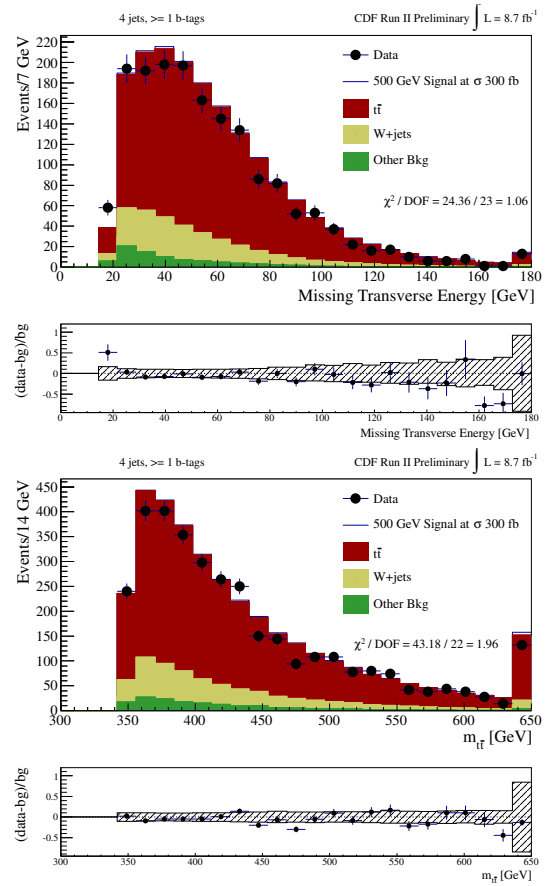


FIG. 5: Validation in the four jet control region: requiring exactly four jets and at least one b -tag.

TABLE II: Expected background and signal and observed yields in the $t\bar{t}$ +jet region, with four jets, at least one b -tag.

CDF Run II Preliminary 8.7 fb^{-1}			
Process	e +jets	μ +jets	total
$t\bar{t}$	616 ± 70	796 ± 90	1410 ± 155
W +jets	122 ± 37	158 ± 48	280 ± 85
Single Top	13 ± 2	15 ± 2	29 ± 4
Z +jets	4 ± 1	7 ± 2	12 ± 2
Diboson	7 ± 2	9 ± 2	16 ± 3
QCD	29 ± 29	< 1	29 ± 29
Total	791 ± 83	986 ± 99	1776 ± 174
Data	812	879	1691
Signal at $\sigma = 300 \text{ fb}$:			
$500 \text{ GeV}/c^2$	8	11	19

APPENDIX: ADDITIONAL MATERIAL

Four jet control region

Table II shows the yields and Figures 4, 5 shows lepton p_T , H_T , \cancel{E}_T and $m_{t\bar{t}}$.

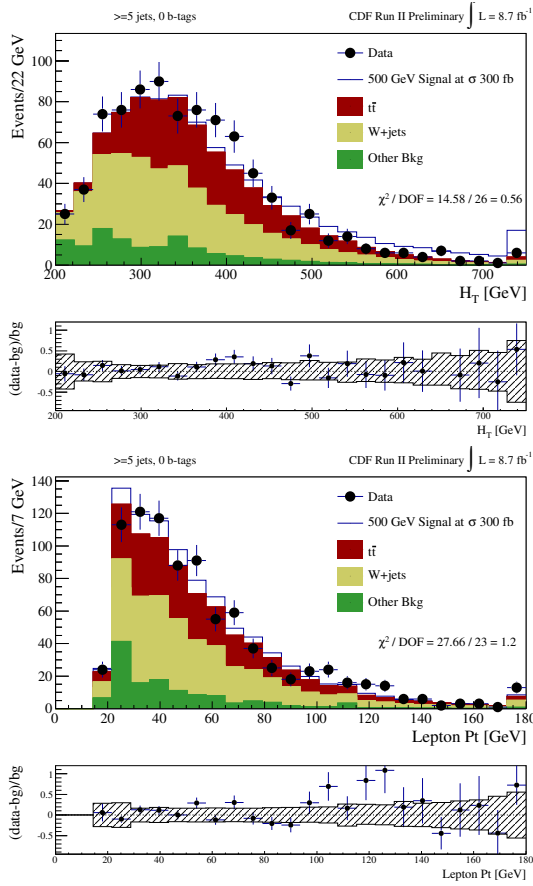


FIG. 6: Validation in the zero b -tag control region: requiring at least five jets and zero b -tags.

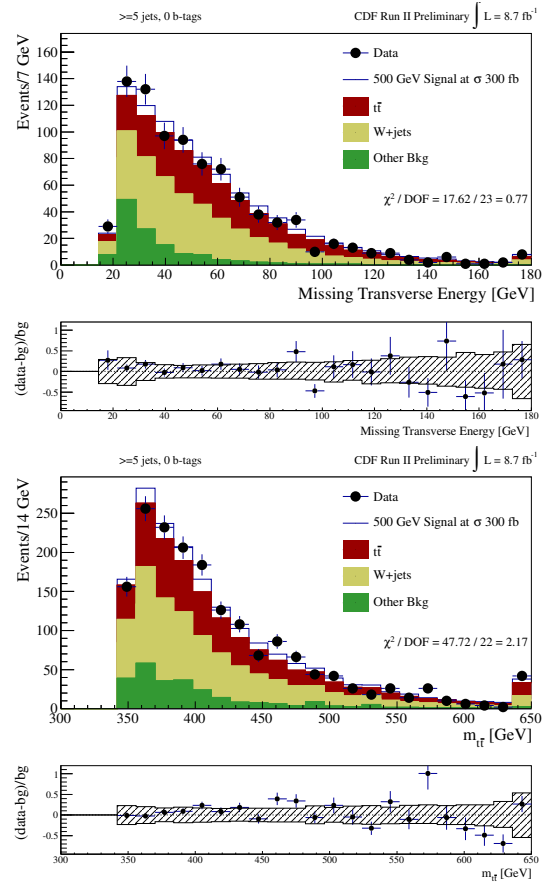


FIG. 7: Validation in the zero b -tag control region: requiring at least five jets and at least one b -tag.

TABLE III: Expected background and signal and observed yields in the $t\bar{t}$ +jet region, with at least five jets, 0 b -tags.

CDF Run II Preliminary 8.7 fb^{-1}			
Process	e +jets	μ +jets	total
$t\bar{t}$	127 ± 30	164 ± 40	291 ± 68
W +jets	184 ± 56	202 ± 61	386 ± 117
Single Top	2 ± 1	2 ± 1	4 ± 1
Z +jets	9 ± 2	12 ± 3	21 ± 4
Diboson	11 ± 3	13 ± 3	24 ± 4
QCD	85 ± 85	< 1	85 ± 85
Total	417 ± 105	393 ± 71	810 ± 135
Data	480	394	874
Signal at $\sigma = 300 \text{ fb}$:			
$500 \text{ GeV}/c^2$	31 ± 1	50 ± 2	81 ± 4

Zero btag control region

Table III shows the yields and Figures 6, 7 shows lepton p_T , H_T , \cancel{E}_T and $m_{t\bar{t}}$.

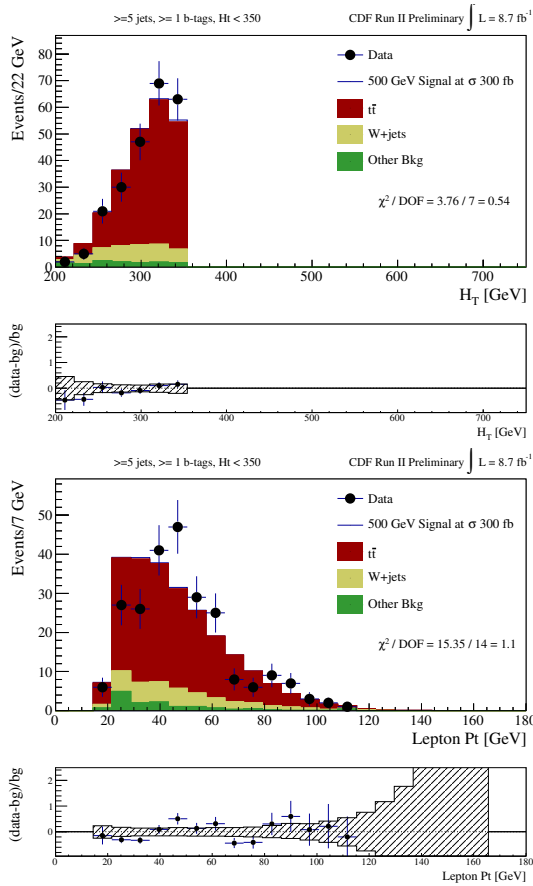


FIG. 8: Validation in the low H_T control region: requiring at least five jets and at least one b -tags and $H_T < 350$.

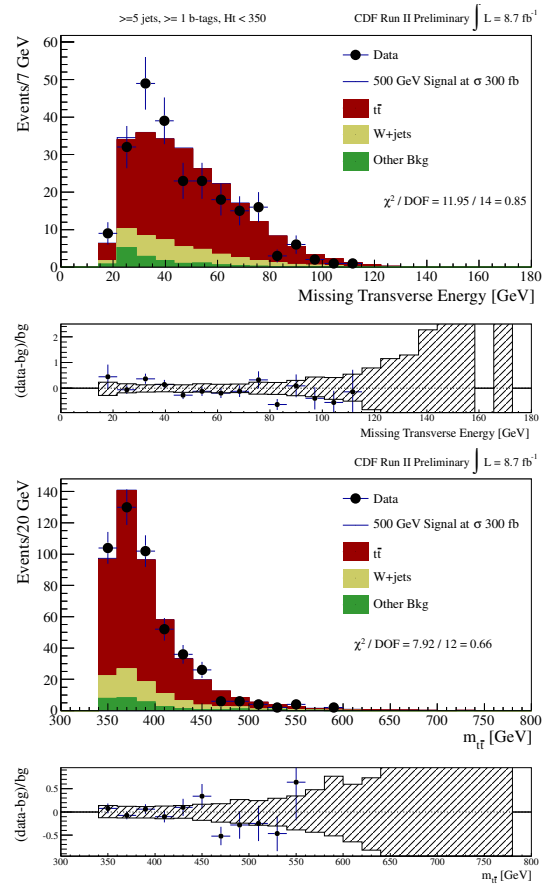


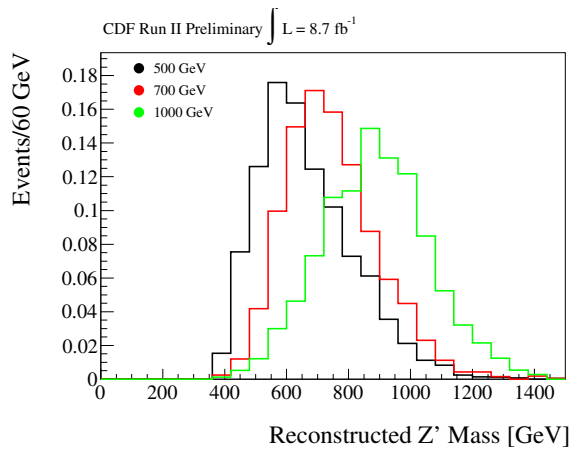
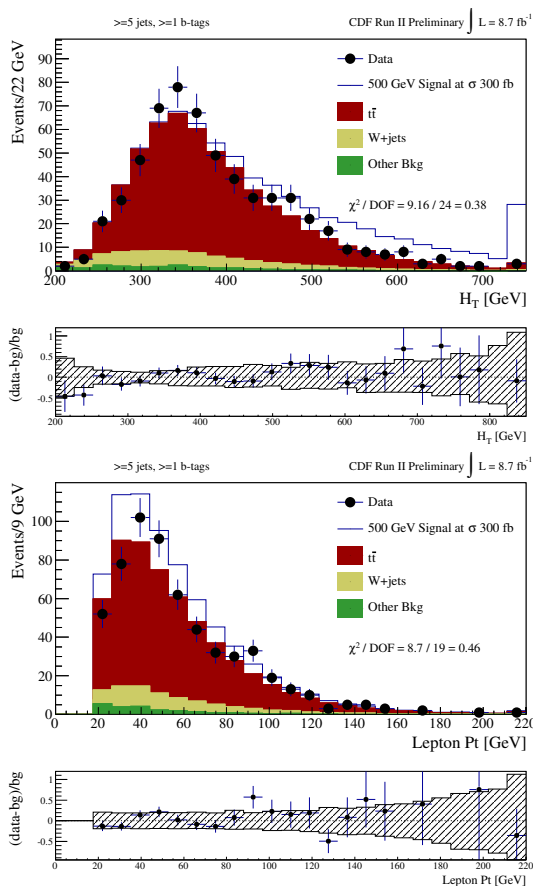
FIG. 9: Validation in the low H_T control region: requiring at least five jets and at least one b -tag and $H_T < 350$.

TABLE IV: Expected background and signal and observed yields in the $t\bar{t}$ +jet region, with at least five jets, at least one b -tag, and $H_T < 350$ GeV.

CDF Run II Preliminary 8.7 fb^{-1}			
Process	e +jets	μ +jets	total
$t\bar{t}$	85 ± 15	107 ± 20	192 ± 30
W +jets	16 ± 6	18 ± 6	34 ± 11
Single Top	1 ± 1	2 ± 1	3 ± 1
Z +jets	0 ± 0	1 ± 1	1 ± 1
Diboson	1 ± 1	1 ± 1	2 ± 1
QCD	8 ± 8	< 1	8 ± 8
Total	112 ± 18	128 ± 20	240 ± 33
Data	108	129	237
Signal at $\sigma = 300 \text{ fb}$:			
$500 \text{ GeV}/c^2$	1	1	2

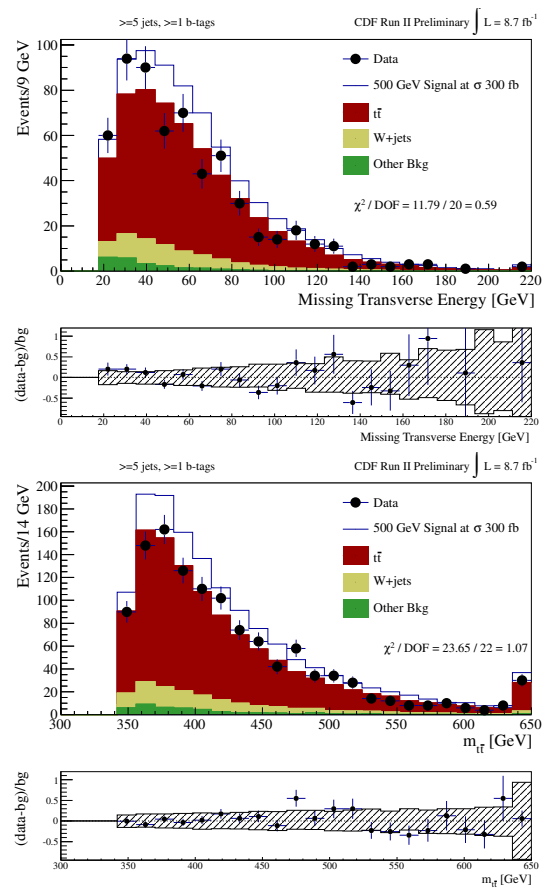
Low HT region

Table IV shows the yields and Figures 8, 9 shows lepton p_T , H_T , \cancel{E}_T and $m_{t\bar{t}}$.

FIG. 10: Reconstructed Z' masses.FIG. 11: Signal region: requiring at least five jets and at least one b -tags .

Signal Region

Figure 10 shows the Z' mass reconstruction in the signal region. Table V shows the yields and Figures 11, 12 shows lepton p_T , H_T , \cancel{E}_T and $m_{\ell\bar{\ell}}$.

FIG. 12: Signal region: requiring at least five jets and at least one b -tag .TABLE V: Expected background and signal and observed yields in the $t\bar{t}$ -jet region, with at least five jets, at least one b -tag.

CDF Run II Preliminary 8.7 fb ⁻¹			
Process	e +jets	μ +jets	total
$t\bar{t}$	206 ± 44	271 ± 61	477 ± 103
W +jets	31 ± 10	36 ± 12	67 ± 21
Single Top	2 ± 1	3 ± 1	6 ± 2
Z +jets	1 ± 1	2 ± 1	3 ± 1
Diboson	2 ± 1	2 ± 1	4 ± 1
QCD	11 ± 11	< 1	11 ± 11
Total	254 ± 47	314 ± 62	568 ± 105
Data	261	325	586
Signal($\sigma = 300$ fb):			
500 GeV/ c^2	55 ± 2	89 ± 4	144 ± 7

- [1] J. Alwall, M. Khader, A. Rajaraman, D. Whiteson and M. Yen, arXiv:1202.4014 (2012).
- [2] CDF Collaboration, Phys. Rev. D **71**, 032001 (2005).
- [3] C. S. Hill, Nucl. Instrum. Methods A **530**, 1 (2004).
- [4] CDF Collaboration, Phys. Rev. Lett. **97**, 082004 (2006);

- CDF Collaboration, Phys. Rev. Lett. **94**, 091803 (2005).
- [5] CDF uses a cylindrical coordinate system with the z axis along the proton beam axis. Pseudorapidity is $\eta \equiv -\ln(\tan(\theta/2))$, where θ is the polar angle relative to the proton beam direction, and ϕ is the azimuthal angle while $p_T = |p| \sin \theta$, $E_T = E \sin \theta$.
- [6] CDF Collaboration, Phys. Rev. D **45**, 001448 (1992).
- [7] A. Bhatti *et al.*, Nucl. Instrum. Methods A **566**, 375 (2006).
- [8] Missing transverse momentum, \cancel{E}_T , is defined as the magnitude of the vector $-\sum_i E_T^i \vec{n}_i$ where E_T^i are the magnitudes of transverse energy contained in each calorimeter tower i , and \vec{n}_i is the unit vector from the interaction vertex to the tower in the transverse (x, y) plane.
- [9] CDF Collaboration, Phys. Rev. D **74**, 072006 (2006).
- [10] J. Alwall *et al.* J. High Energy Phys. **0709** (2007) 028.
- [11] T. Sjostrand *et al.*, Comput. Phys. Commun. **238**, 135 (2001), version 6.422.
- [12] E. Gerchtein and M. Paulini, arXiv:physics/0306031 (2003).
- [13] Electroweak Working Group (CDF and D0 Collaborations), arXiv:1107.5255 [hep-ex] (2011). We use a top-quark mass of $172.5 \text{ GeV}/c^2$ which is within errors of the current Tevatron combination of $173.2 \pm 0.9 \text{ GeV}/c^2$.
- [14] U. Langenfeld *et al.*, Phys. Rev. D **80**, 054009 (2009).
- [15] S. Frixione, P. Nason, and B. Webber, J. High Energy Phys. **08**, 007 (2003).
- [16] M. Mangano *et al.*, J. High Energy Phys. **0307** (2003) 001.
- [17] J. Campbell and R. Ellis, Phys. Rev. D **60**, 113006 (1999).
- B. W. Harris *et al.*, Phys. Rev. D **66**, 054024 (2002).
- [18] CDF Collaboration, Phys. Rev. D. **73**, 32003 (2006).
- [19] A. Read, Nucl. Instrum. Methods A **425**, 357 (1999).
- [20] A. Read, J. Phys. G: Nucl. Part. Phys. **28**, 2693 (2002); T. Junk, Nucl. Instrum. Methods A **434**, 425 (1999).
- [21] ATLAS Collaboration, <https://atlas.web.cern.ch/Atlas/GROUPS/PHYSICS/CONFNOTES/ATLAS-CONF-2012-007/>
- [22] CMS Collaboration, <https://twiki.cern.ch/twiki/bin/view/CMSPublic/PhysicsResultsEX011019Winter2012>
- [23] CMS Collaboration, arXiv:1204.2488 [hep-ex] (2012)
- [24] ATLAS Collaboration, <https://atlas.web.cern.ch/Atlas/GROUPS/PHYSICS/CONFNOTES/ATLAS-CONF-2012-029/>